

# Underflight Calibration of SOHO CDS by SERTS-97

ROGER J. THOMAS

*Laboratory for Astronomy and Solar Physics  
NASA Goddard Space Flight Center  
Greenbelt, MD, USA*

Flights of the SERTS sounding rocket were made in 1997, 1999, and 2000 to provide updated radiometric and wavelength calibrations for several experiments on the SOHO satellite mission. Just before or after each of these flights, end-to-end radiometric calibrations of the rocket payload were carried out using an EUV transfer standard light-source specially re-calibrated against the primary standard of BESSY I. These measurements established the absolute SERTS responsivity within a relative uncertainty of 17 % over its bandpass of 30 nm to 36 nm. During the flights, SERTS and SOHO CDS observed the same solar locations, as demonstrated by subsequent data co-registration with simultaneous SOHO EIT images, allowing the SERTS calibrations to be directly applied to both CDS and EIT. Following is a brief summary of the SERTS-97 radiometric calibration and the underflight cross-calibration that it provided for the CDS NIS channels at a time shortly before SOHO's temporary loss of pointing control.

## 14.1 Introduction

The Solar EUV Research Telescope and Spectrograph (SERTS) developed by the Goddard Space Flight Center (GSFC) is a rocket instrument that obtains imaged high-resolution spectra of individual solar features to study the Sun's corona and upper transition region. Flights in 1997, 1999, and 2000 also provided radiometric and wavelength calibrations for several experiments on the SOHO satellite mission. For that purpose, end-to-end radiometric calibrations of SERTS were carried out just before or after each flight in the same facility that had been used to characterize the SOHO CDS experiment at Rutherford Appleton Laboratory (RAL) [Lang *et al.*, 2000, 2002], and using the same EUV light source specially re-calibrated against the primary EUV radiation standard of BESSY I. These measurements can establish the absolute SERTS responsivity within a relative standard uncertainty of 25 % or better at 12 wavelengths covering its bandpass of 30 nm to 36 nm. Post-flight wavelength calibrations were done at GSFC using laboratory standard lines of He II and Ne II. Each SERTS payload also carried an EUV solar flux monitor kindly provided by the University of Southern California (USC) [McMullin *et al.*, 2002]; its readings were used to validate calculations of atmospheric EUV transmission over the rocket's trajectory, and to provide an updated calibration for SOHO CELIAS. During each flight, SERTS and CDS observed the same solar locations, as demonstrated by subsequent

data co-registration with simultaneous SOHO EIT images, allowing the SERTS calibrations to be directly applied to both CDS and EIT. Following is a brief summary of the SERTS-97 radiometric calibration and the underflight cross-calibration that it provided for the CDS NIS-1 and NIS-2 channels, a few months before SOHO's loss of pointing control in 1998.

## 14.2 Calibration Source - EUV Transfer Standard

To support SOHO, the Physikalisch-Technische Bundesanstalt (PTB) developed a special EUV radiometric transfer standard, based on a hollow cathode lamp combined with collimating optics [Hollandt *et al.*, 2002]. Different gasses can be fed through the hollow cathode to provide radiation from a wide variety of emission lines. Controls for the operating conditions of the lamp ensure that its output is stable and repeatable. The lamp's exit aperture is a 0.6 mm-diameter pinhole positioned at the focal point of an inverted grazing-incidence Wolter Type-II telescope, which had been made by GSFC for the SERTS program, then donated to PTB. A collimated beam emerges from the telescope, and is limited to a diameter of 5 mm by a final aperture. The entire device is mounted on a table that can be moved and tilted in a controlled manner.

This source was characterized by PTB against the BESSY I electron storage ring, a primary radiometric standard, and used to carry out the pre-launch calibrations of the SOHO CDS experiment. In 1995, the source was again specially re-characterized directly against BESSY I for the SERTS project over the spectral bandpass of 26 nm to 38 nm. These later measurements demonstrated that the source showed no systematic degradation over the several-year period involved, and that its absolute radiant power at each wavelength could be established to within a relative standard uncertainty of 7 %. Table 14.1 lists the final results of all such BESSY runs with the transfer source for the wavelengths used to calibrate the SERTS instrument, at 11 sets of lines between 30 nm to 36 nm by using neon, and at 30.38 nm by using helium. Further details of this source and its calibration are given by Hollandt *et al.* [2002].

## 14.3 SERTS-97 Radiometric Calibration

In September 1997, the SERTS rocket payload was shipped to RAL and installed in the same vacuum chamber that had been used to carry out the pre-launch calibrations of the SOHO CDS instrument. The calibration source described above was then attached and aligned to the SERTS optical axis by means of a red laser shining through the source optics. This laser was adjusted to retro-reflect from the SERTS reference mirror, and its position was set to illuminate a specific target point on the SERTS telescope aperture. In that orientation, a spotting telescope attached to the source table was locked into position sighting a corresponding target point on a map of the SERTS aperture that was attached to the side of the rocket payload. In addition, an auto-collimator, also attached to the source, was locked into position viewing the reflection from a large flat mirror that was fixed to the other side of the SERTS instrument. These both looked through window ports in the vacuum chamber's door, so that the relative position and tilt between the source and instrument could always be controlled during the calibration runs. Flexible bellows in the

Table 14.1: Radiant power and photon flux of the EUV transfer-standard source. Results are mean values of all calibration periods.

Emission Lines / nm	Integration Range / nm	Spectrum	Radiant Power / pW	Photon Flux / s <sup>-1</sup>	Rel. Std. Uncert.
30.11	29.95-30.25	Ne III	10.4	$1.58 \cdot 10^6$	7 %
30.38	29.90-30.90	He II	319.0	$4.88 \cdot 10^7$	7 %
30.48/30.55	30.35-30.65	?	6.71	$1.03 \cdot 10^6$	7 %
30.86	30.75-31.00	Ne III	4.10	$6.37 \cdot 10^5$	7 %
31.31-31.39	31.20-31.55	Ne III	12.4	$1.96 \cdot 10^6$	7 %
31.95/32.00	31.80-32.15	?	11.6	$1.87 \cdot 10^6$	7 %
32.46/32.54	32.35-32.57	Ne II	4.34	$7.10 \cdot 10^5$	7 %
32.65-32.81	32.57-32.82	Ne II	38.4	$6.36 \cdot 10^6$	7 %
33.01-33.15	32.82-33.35	Ne II	21.3	$3.53 \cdot 10^6$	7 %
35.22-35.39	35.00-35.40	Ne II	17.7	$3.17 \cdot 10^6$	7 %
35.50-35.75	35.40-35.85	Ne II	59.3	$1.06 \cdot 10^7$	7 %
36.14/36.25	35.95-36.45	Ne II	43.0	$7.84 \cdot 10^6$	7 %

vacuum pipe connecting the source to the vacuum chamber permitted the needed motions and tilts. In order to assure that all source radiation reached the detector, the slit of the SERTS spectrometer was removed. The entrance aperture of the SERTS-97 instrument is

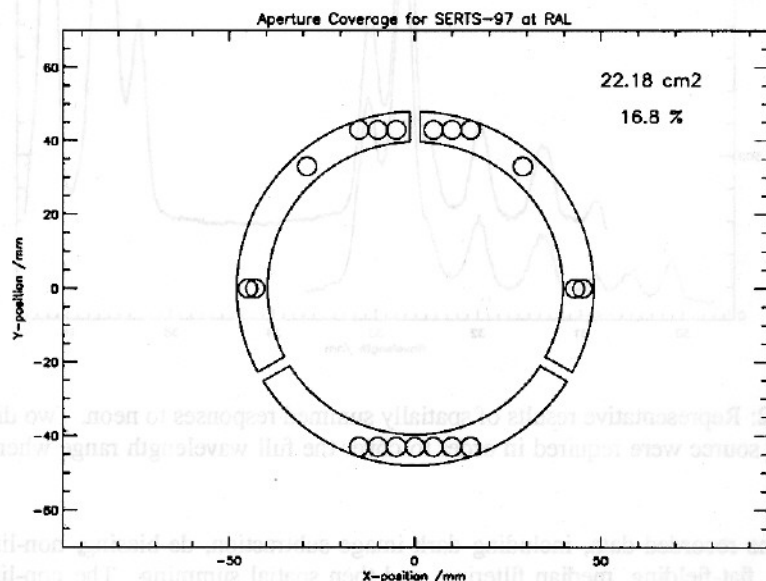


Figure 14.1: The entrance aperture of the SERTS-97 instrument. Smaller circles show the areas illuminated by the narrow beam of the EUV calibration source.

an annulus with inner and outer radii of 39.70 mm and 48.01 mm, and with three spider-arms each 2.87 mm wide. Various parts of the aperture are illuminated by translating the

narrow source-beam relative to the payload. Horizontal translation is accomplished by a motorized table inside the vacuum chamber on which the payload is mounted, while vertical translation is done by jacking the source-table up and down. A total of nineteen locations within the instrument aperture were covered with the 5 mm-diameter beam in this way, representing 16.8 % of its full area (Figure 14.1).

SERTS-97 used an intensified CCD detector with a  $3072 \times 2048$  array of 9-micron pixels<sup>1</sup>, cooled to  $-20^\circ\text{C}$ . For each entrance aperture location, this detector recorded a spectrally dispersed image of the 0.6 mm source pinhole in the various emission lines being emitted. Since all of the useful neon lines could not fit onto the detector in one image, two different tilts of the source were required in order to cover the full wavelength range when using that gas. Representative results of spatially summed responses to neon are shown in Figure 14.2, in which the eleven measured spectral features can be seen. Although some of these features appear blended, their separate contributions can be reliably determined by fitting multiple Gaussians to the overall profiles. Several routine adjustments are applied

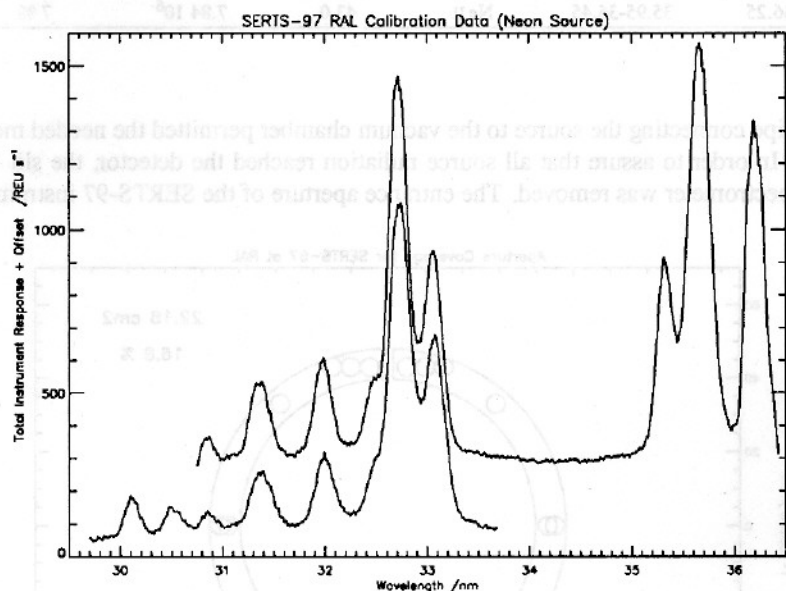


Figure 14.2: Representative results of spatially summed responses to neon. Two different tilts of the source were required in order to cover the full wavelength range when using that gas.

to all of the recorded data, including dark image subtraction, de-biasing, non-linearity correction, flat-fielding, median filtering, and then spatial summing. The non-linearity correction is determined by comparing data that differ only by exposure time, and is used to convert the raw recorded Data Numbers (DN) to Relative Exposure Units (REU). The total response rate in REU/s at each wavelength is then found by Gaussian fits to all 99 of the corrected calibration images, taken on ten days during the full run of three weeks. Since a given wavelength feature was recorded multiple times, the values of those readings

<sup>1</sup> 1 micron =  $1\ \mu\text{m} = 10^{-6}\text{m}$

were averaged for each entrance aperture position measured, and then averaged again over all aperture positions to simulate full-aperture illumination.

The final calibration is shown in Figure 14.3, which gives the measured SERTS-97 absolute end-to-end response in units of REU/erg as a function of wavelength. The peaked

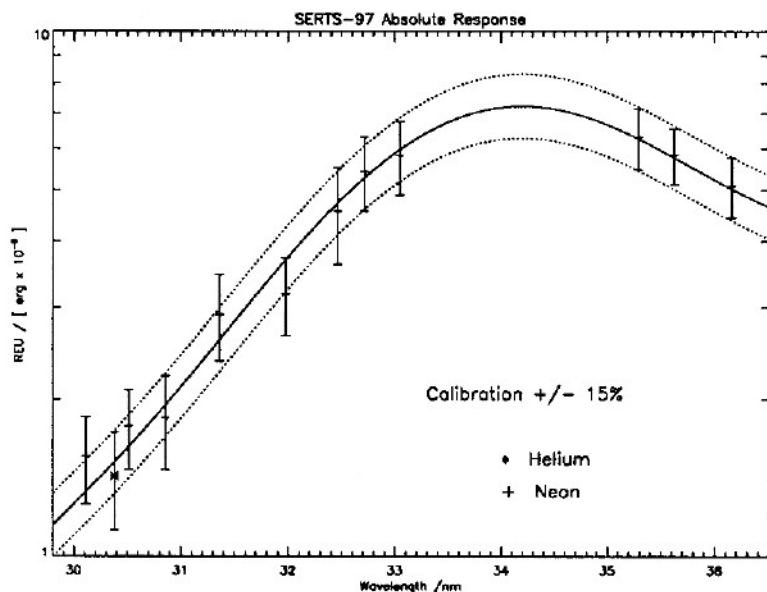


Figure 14.3: SERTS-97 absolute end-to-end response in Relative Exposure Units (REU) per erg as a function of wavelength. Error-bars show the total range of values measured from the different sub-aperture positions.

shape of the curve is mainly due to the multilayer coating on the spectrograph grating, which was applied to enhance its EUV efficiency. Error-bars reflect the total range of values measured from the various entrance aperture positions. The solid line is a Gaussian plus slope, which represents the measurements to well within the 15 % uncertainty limits shown. This response curve giving  $\text{Resp}/\text{Srce}$  is then used with the following relationships

$$\begin{aligned} \text{Cal} &= \text{Srce} \times (\text{K}/\text{PScl})^2 / \text{Area} / \text{Resp} \\ \text{Lobe Calibration} &= \text{Cal} / \text{Pix}^2 \\ \text{Slit Calibration} &= \text{Cal} / \text{Pix} / \text{Slit} \end{aligned}$$

and with the various geometric values given in Table 14.2 to determine the appropriate calibration factors for SERTS observations made either with its narrow slit or with its wide lobe. In the table, Slit is the width of the spectrometer's narrow slit, and Area refers to the instrument's entrance aperture; both were measured with an accurate travelling microscope. Pix is the detector pixel size, taken from manufacturer's specifications. PScl is the spatial Plate Scale of the instrument, which was determined by cross-correlations of SERTS lobe data against simultaneous EIT images, both at 30.4 nm [Thompson, 1999]. This was done in units of SOHO-arcsec/SERTS-pixel, and so requires conversion by the

Table 14.2: SERTS-97 calibration conversion

Calibration Factors		Units	Rel. Std. Uncert.
Resp	Resp( $\lambda$ )	REU / s	15.0 %
Srce	Srce( $\lambda$ )	erg / s	7.0 %
Slit	21.5	$\mu\text{m}$	2.0 %
Area	22.18	$\text{cm}^2$	1.0 %
PScl	$0.7869 / 9 \times 1.00282$	" / $\mu\text{m}$	0.2 %
Pix	9.0	$\mu\text{m}$	0.0 %
K	$180 \times 60 \times 60 / \pi$	" / rad	0.0 %

factors of 1.00282 1AU-arcsec/SOHO-arcsec, and of 9  $\mu\text{m}$ /SERTS-pixel. Finally, K is just the number of arcsec per radian. The resulting relative standard uncertainty of Cal (which has units of  $\text{erg cm}^{-2} \text{sr}^{-1} \text{REU}^{-1} \mu\text{m}^2$ ) is 17 %.

## 14.4 CDS Underflight Calibration

On 18 November 1997 at 1935 UT, the calibrated SERTS payload was launched from White Sands Missile Range, New Mexico, and made imaged spectral observations of active region NOAA-8108 on the solar disk at heliographic coordinates N21E18. Starting a few hours before this flight and ending a few hours after it, the CDS instrument on SOHO observed the same solar target with spectral coverage that included the SERTS bandpass. Cross-correlations of the resulting images at He II 30.4 nm with the full-disk image from SOHO EIT allowed all three to be spatially co-registered to within 1.8". The alignment was verified by comparing spatial distributions of the highly variable Fe XVI 33.5 nm emission measured by both SERTS and CDS, which showed excellent relative agreement. A 30" area along the SERTS slit was not used in the cross-calibration because a small sub-flare there caused too much time variability. However, on the remaining area of overlap between the CDS raster-field and the SERTS slit (190"), all consecutive observations agree within 2 %.

In addition to the standard data-reduction procedures mentioned in the previous Section, two other corrections were applied to the SERTS flight data. The first was an adjustment for atmospheric extinction at rocket altitudes, which was computed using radar measurements of the flight trajectory and the MSIS-86 model of the Earth's neutral thermosphere [Hedin, 1987]. SERTS-97 carried a full-disk EUV monitor provided by USC, whose measurements showed that atmospheric extinction is indeed well-fitted by the MSIS model used, and in any case is less than 10 % for all but two of the SERTS exposures. The second correction was to reduce instrumental line-profile distortions by applying two iterations of LUCY, a SolarSoft IDL routine based on image restoration methods described by Richardson [1972] and by Lucy [1974]. Pre-flight laboratory images were used to provide the instrumental point-spread function for that correction. The CDS measurements were likewise treated with their standard data-reduction routines, except that no radiometric factors were applied so that they were left in raw units of detector photon-events.



Both SERTS and CDS data were then spatially averaged over their area of overlap, excluding the sub-flare, giving the spectral curves shown in Figure 14.4. Here the SERTS

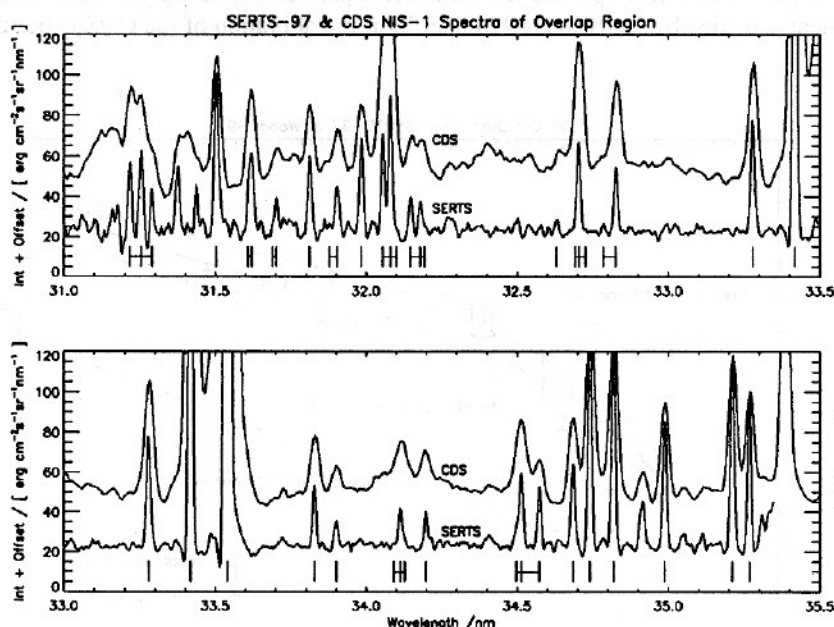


Figure 14.4: Comparison of SERTS and CDS NIS-1 spectral measurements made on 18 November 1997, spatially averaged over the same areas of the solar disk. The 26 spectral features used in the NIS-1 cross-calibration are indicated.

measurements are in absolute units, while the CDS data have been scaled to match; both have arbitrary offsets to show the curves more clearly. All line intensities were found by Gaussian fits relative to the local background. Those indicated by vertical bars were strong and clean enough to be used in the cross-calibration. Since the CDS spectral resolution is somewhat poorer than that of SERTS, a number of lines had to be grouped in the comparison, but this still allowed valid cross-calibrations at a total of 26 wavelengths in the CDS NIS-1 channel, and another two (second spectral-order) wavelengths in CDS NIS-2.

The final results are summarized in Figure 14.5. The error-bars here represent line-fitting uncertainties only, and do not include the effect of uncertainty in the SERTS absolute calibration. The Figure includes an additional point at 36.8 nm from the Woods-97 rocket flight [Brekke *et al.*, 2000], which seems to agree well with an extension of the SERTS results. The polynomial fit (solid line) matches nearly every point to within 15 %, as indicated by the close dotted lines on either side. This curve has been implemented in SolarSoft as the current CDS NIS-1 calibration, through the following relationships:

$$\begin{aligned} \text{Response} &= \text{poly}(\text{Wave}, \text{Coef}) \\ \text{Coef} &= [-1.88868822, 0.166374198, -0.00490782871, 4.86757761\text{e-}05] \end{aligned}$$

where poly is the IDL-library routine for evaluating polynomial functions. The listed values of Coef give the CDS NIS-1 conversion factor, Response, in units of photon events

per ( $\text{erg cm}^{-2} \text{sr}^{-1}$ ) when the variable wavelengths, Wave, are input in units of nm. Also shown is the previous calibration curve used for CDS NIS-1 [Landi *et al.*, 1997], as well as the original curve from pre-launch measurements, demonstrating the significant improvement provided by the SERTS-97 underflight re-calibration of the CDS experiment.

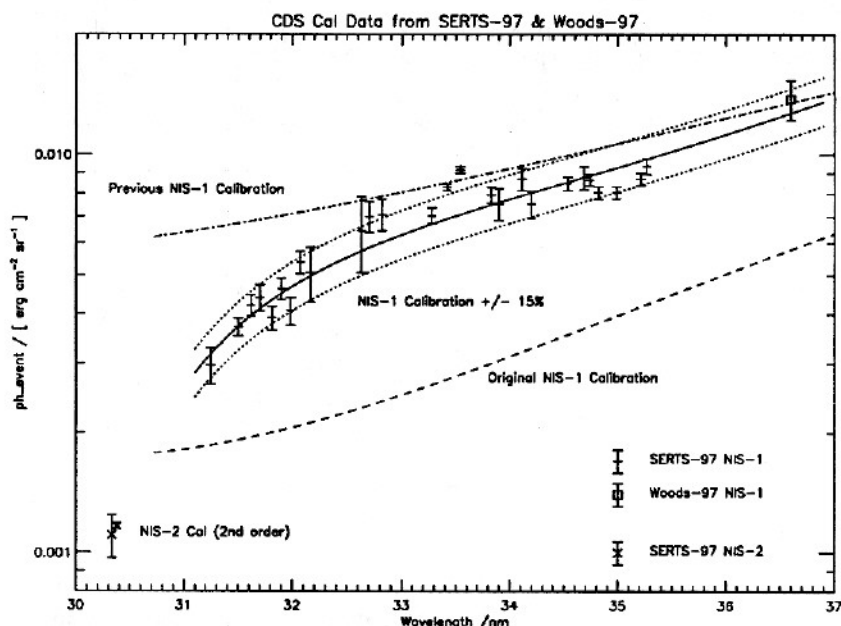


Figure 14.5: The ratio of CDS intensities in detector photon-event units to those measured by SERTS-97 in absolute units. Two points at 30.3 and 30.4 nm are for the second spectral order of NIS-2; all others are for first-order NIS-1. See the text for explanations of the various curves.

## Acknowledgements

The PTB transfer source was developed under the leadership of Michael Kühne, while its characterization at BESSY I and operation at RAL were primarily done by Jörg Hollandt. SERTS calibrations at RAL depended on the tireless efforts of Barry Kent, and on the constant support of Richard Harrison. Much of the SERTS software, as well as CDS cross-calibration operations and data reduction, were carried out by William Thompson. The SERTS rocket project, initiated by Werner Neupert, has been led over the past twelve years by Joseph Davila. Heartfelt thanks are extended to Jim Lang, William Thompson, and especially to Anuschka Pauluhn for their many helpful suggestions and patient editing of the present manuscript. This work is funded by NASA RTOPs 370-18-37 and 344-17-38.



## Bibliography

- Brekke, P., Thompson, W.T., Woods, T.N., and Eparvier, F.G., The extreme-ultraviolet solar irradiance spectrum observed with the Coronal Diagnostic Spectrometer (CDS) on SOHO, *Astrophys. J.* **536**, 959–970, 2000.
- Hedin, A.E., MSIS-86 Thermospheric Model, *J. Geophys. Res.* **92**, 4649–4662, 1987.
- Hollandt, J., Kühne, M., Huber, M.C.E., and Wende, B., Source standards for radiometric calibration of astronomical telescopes in the VUV spectral range traceable to the primary standard BESSY, this volume, 2002.
- Landi, E., Landini, M., Pike, C.D., and Mason, H.E., SOHO CDS-NIS in-flight intensity calibration using a plasma diagnostic method, *Sol. Phys.* **175**, 553–570, 1997.
- Lang, J., Kent, B.J., Breeveld, A.A., Breeveld, E.R., Bromage, B.J.I., Hollandt, J., Payne, J., Pike, C.D., and Thompson, W.T., The laboratory calibration of the SOHO Coronal Diagnostic Spectrometer, *J. Opt. A: Pure Appl. Opt.* **2**, 88–106, 2000.
- Lang, J., Thompson, W.T., Pike, C.D., Kent, B.J., and Foley, C.R., The calibration of the Coronal Diagnostic Spectrometer, this volume, 2002.
- Lucy, L.B., An iterative technique for the rectification of observed distributions, *Astronomical J.* **79**, 745–754, 1974.
- McMullin, D.R., Judge, D., Hilchenbach, M., Ipavich, F., Bochsler, P., and Bürgi, A., In-flight comparisons of solar EUV irradiance measurements provided by the CELIAS/SEM on SOHO, this volume, 2002.
- Richardson, W.H., Bayesian-based iterative method of image restoration, *Journal of the Optical Society of America* **62**, 55–59, 1972.
- Thompson, W.T., personal communication, 1999.

SEFRTS(C) Toroid .txt

Tel: EFL=2120.0, PFL= 714.0, FNO= 22.0, FNI= 30.5, Az= 0, REX=360  
 Tel Spot = 20.0, slit width = 20.0, Detector Blur = 13.0 [um]  
 Ro[mm] = 1150.00 Alp[d] = 7.011 b2 = 0.00000  
 Rs[mm] = 1200.02 L[/mm] = 3600.0 b3 = 0.00000  
 Rt[mm] = 1209.67 b4 = 0.00000  
 Flat: Xint[mm], Slope = 124.933 -0.127548

Lambda	[A]	DYMA DZsec	DYum	DZum	Eta	Z'	Y'	X'	R'
298.0	56	2.3	25.7	25.9	0	-0.00	172.91	102.88	1264.75
303.6	56	2.3	25.8	25.9	0	0.00	170.38	103.20	1264.73
309.2	57	2.3	26.0	26.0	0	0.00	167.85	103.52	1264.71
314.8	57	2.3	26.1	26.0	0	0.00	165.32	103.85	1264.70
320.4	57	2.3	26.3	26.1	0	-0.00	162.79	104.17	1264.69
326.0	57	2.3	26.4	26.1	0	-0.00	160.27	104.49	1264.69
331.6	58	2.3	26.4	26.2	0	0.00	157.74	104.81	1264.69
337.2	57	2.3	26.4	26.3	0	-0.00	155.21	105.14	1264.70
342.8	57	2.3	26.3	26.3	0	-0.00	152.68	105.46	1264.71
348.4	57	2.3	26.2	26.4	0	0.00	150.15	105.78	1264.73
354.0	57	2.3	26.0	26.5	0	0.00	147.62	106.10	1264.75

# Ray-Trace Toroidal Grating Spectrograph

Eta[sec] = 0

Tel: EFL=2120.0, PFL= 714.0, FNo= 22.0, FNi= 30.5, Az= 0, Rex=360

Tel Spot = 20.0, Slit Width = 20.0, Detector Blur = 13.0 [um]

Flat: Xint[mm], Slope = 124.933 -0.127548

..... Spatial  
 ——— Spectral

RMS Spot Diameter [um]

25  
20  
15  
10  
5  
0

300

310

320

Wavelength [A]

330

340

350

ro=1150.00mm

Rs=1200.02mm

Rt=1209.67mm

Al= 7.011deg

ld=3600/mm

b2= 0.00000

b3= 0.00000

b4= 0.00000